JCB Article

Phospholipids undergo hop diffusion in compartmentalized cell membrane

Takahiro Fujiwara,[1] Ken Ritchie,[1,2] Hideji Murakoshi,[2] Ken Jacobson,[3] and Akihiro Kusumi[1,2]

[1]Kusumi Membrane Organizer Project, Exploratory Research for Advanced Technology Organization (ERATO), Japan Science and Technology Corporation, Nagoya 460-0012, Japan
[2]Department of Biological Science, Nagoya University, Nagoya 464-8602, Japan
[3]Department of Cell and Developmental Biology and Lineberger Comprehensive Cancer Center, University of North Carolina, Chapel Hill, NC 27599

Downloaded from http://rupress.org/jcb/article-pdf/157/6/1071/1304489/jcb157761071.pdf by guest on 28 September 2022

The diffusion rate of lipids in the cell membrane is reduced by a factor of 5–100 from that in artificial bilayers. This slowing mechanism has puzzled cell biologists for the last 25 yr. Here we address this issue by studying the movement of unsaturated phospholipids in rat kidney fibroblasts at the single molecule level at the temporal resolution of 25 μs. The cell membrane was found to be compartmentalized: phospholipids are confined within 230-nm-diameter (ϕ) compartments for 11 ms on average before hopping to adjacent compartments. These 230-nm compartments exist within greater 750-nm-ϕ compartments where these phospholipids are confined for 0.33 s on average. The diffusion rate within 230-nm compartments is 5.4 $\mu m^2/s$, which is nearly as fast as that in large unilamellar vesicles, indicating that the diffusion in the cell membrane is reduced not because diffusion per se is slow, but because the cell membrane is compartmentalized with regard to lateral diffusion of phospholipids. Such compartmentalization depends on the actin-based membrane skeleton, but not on the extracellular matrix, extracellular domains of membrane proteins, or cholesterol-enriched rafts. We propose that various transmembrane proteins anchored to the actin-based membrane skeleton meshwork act as rows of pickets that temporarily confine phospholipids.

Introduction

For the past 25 yr, one of the most serious puzzles in the research of membrane dynamics is how the diffusion rate of lipids in the cell membrane is reduced by a factor of 5–100 from that in artificial bilayers (Swaisgood and Schindler, 1989; Lee et al., 1993; Ladha et al., 1996; Sonnleitner et al., 1999). Long-range interactions between lipids and immobilized proteins (Sperotto and Mouritsen, 1991; Almeida et al., 1992; Bussell et al., 1995; Dodd et al., 1995) or interactions with the extracellular matrix (Wier and Edidin, 1986; Lee et al., 1993) may be responsible for such a reduction of lipid diffusion rates. Alternatively, cholesterol-enriched lipid microdomains called "rafts" (for reviews see Simons and Toomre, 2000; Edidin, 2001) may be involved in such a slowing mechanism by inducing partitioning of raft lipids into raft domains or by becoming diffusion obstacles for nonraft lipids.

To address the problem of slowed lipid diffusion and to acquire a better general understanding of the dynamic lipid organization in the cell membrane, we observed the movement of phospholipids at the single molecule level at a very high time resolution (up to 25 μs), which turned out to be absolutely necessary to elucidate such a slowing mechanism. As a test molecule, we used 1,2-dioleoyl-*sn*-glycero-3-phosphoethanolamine (DOPE),* which is a typical nonraft lipid. Such an unsaturated phospholipid is thought to be most difficult to have its diffusion rate reduced in the cell membrane. DOPE diffusion as observed at 25-μs resolution revealed that the cell membrane is compartmentalized with regard to translational diffusion of DOPE. A DOPE molecule is confined within a 230-nm compartment for 11 ms on average before hopping to an adjacent compartment, and by repeating such temporary confinement and intercompartmental hop movement, it undergoes macroscopic diffusion over many

The online version of this article includes supplemental material.

Address correspondence to Akihiro Kusumi, Department of Biological Science, Nagoya University, Nagoya 464-8602, Japan. Tel.: 81-52-789-2969. Fax: 81-52-789-2968. E-mail: akusumi@bio.nagoya-u.ac.jp

Key words: cell membrane; phospholipid; hop diffusion; single particle tracking; membrane skeleton

*Abbreviations used in this paper: ϕ, diameter; D_{MACRO}, macroscopic diffusion coefficient; D_{micro}, microscopic diffusion coefficient; DOPE, 1,2-dioleoyl-*sn*-glycero-3-phosphoethanolamine; LUV, large unilamellar vesicle; MSD, mean square displacement; NRK, normal rat kidney fibroblastic cell; SPT, single particle tracking; TfR, transferrin receptor.

© The Rockefeller University Press, 0021-9525/2002/06/1071/11 $5.00

compartments. The DOPE diffusion rate within a 230-nm compartment is 5.4 $\mu m^2/s$, which is nearly as fast as that in large unilamellar vesicles, suggesting that DOPE undergoes free diffusion within 230-nm compartments. In contrast, macroscopic diffusion of DOPE over many compartments is much slower, indicating that the diffusion in the cell membrane is reduced not because diffusion per se is slow in the cell membrane, but because the cell membrane is compartmentalized with regard to the lateral diffusion of phospholipids.

We then investigated how such compartmentalization occurs. The results were quite unexpected: such compartmentalization does not depend on the extracellular matrix, extracellular domains of membrane proteins, or rafts, but on the actin-based membrane skeleton, which is located on the cytoplasmic surface of the cell membrane. It is concluded that the various transmembrane proteins anchored to the actin membrane skeleton meshwork act as rows of pickets due to the effects of both steric hindrance and the circumferential slowing. Circumferential slowing is caused by the increased packing near the protein (in terms of the free volume theory) (Sperotto and Mouritsen, 1991; Almeida et al., 1992) or by the increased hydrodynamic friction (in terms of the hydrodynamic theory) (Bussell et al., 1995; Dodd et al., 1995). These anchored-protein pickets temporarily confine phospholipids. Such compartmentalization may be necessary for localization of intracellular signals at the point where the extracellular signal has been received.

Results

Both single fluorophore video imaging and single particle tracking of DOPE molecules in a 100-ms time window showed the same diffusion rate of ~0.5 $\mu m^2/s$, which is smaller by a factor of ~20 than that in artificial bilayers

DOPE was tagged with Cy3 in the head group region and was incorporated into the cell membrane of normal rat kidney (NRK) fibroblastic cells, and these Cy3–DOPE molecules were observed individually under an objective lens-type total internal reflection fluorescence microscope at 37°C at the video rate (33-ms resolution; Fig. 1 A; Video 1 available at http://www.jcb.org/cgi/content/full/jcb.200202050/DC1). The diffusion coefficients in a 100-ms time window (obtained for a period of 100 ms; D_{100ms}) and in a 3-s time window (D_{3s}; Fig. 1 B) were 0.41 and 0.42 $\mu m^2/s$ on average, respectively. The predominant freely diffusing behavior of Cy3–DOPE molecules in this time scale is consistent with the single dye tracing results of Cy5–DOPE by Schütz et al. (2000). These values, however, were found to be smaller by a factor of ~20 than those in artificial bilayers (Table I). Such slowing of diffusion suggests the presence of mechanisms for hampering the lipid movement in the cell membrane, mechanisms that cannot be resolved at the video rate.

Because achieving higher time resolutions in single fluorophore observations is difficult due to the problem of low signal-to-noise ratios, we employed a single particle tracking (SPT) technique of binding a 40-nm-diameter (ϕ) colloidal gold particle to a DOPE molecule in the cell membrane (Video 1). SPT provides higher signal intensities that allow high-speed observations, whereas single fluorophore video imaging of Cy3–DOPE has the advantage that a single fluorescent spot represents a single molecule. The movement of DOPE–gold complexes was examined by contrast-enhanced optical microscopy at 37°C recorded by a high-speed video camera with a temporal resolution of 25 μs (a spatial precision of 17 nm at this recording rate). Labeling conditions were optimized by adjusting the concentration of fluorescein–DOPE incubated with the cells and the amount of Fab fragments conjugated with the gold particles, so that the effect of cross-linking by gold particles was minimized while sufficient specificity in binding of the gold particles was maintained.

D_{3s} (3-s time window) observed was 0.17 $\mu m^2/s$, which was smaller by a factor of 2.5 than that of single Cy3–DOPE molecules (0.42 $\mu m^2/s$), suggesting a moderate steric or cross-linking effect of gold particles on long-range diffusion. However, D_{100ms} (100-ms time window) under this condition was 0.49 $\mu m^2/s$. This value agrees with that of Cy3–DOPE (0.41 $\mu m^2/s$), indicating that the labeling with colloidal gold did not affect the movement of DOPE in shorter time windows,

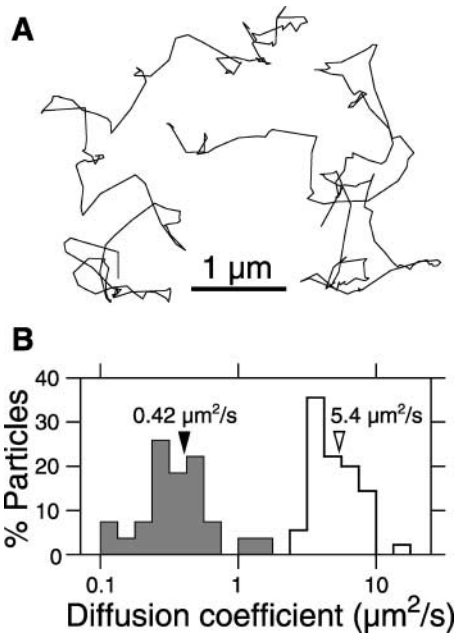

Figure 1. **Phospholipid macroscopic diffusion in the cell membrane is slowed by a factor of ~20 from that in LUV membranes.** (A) Two representative trajectories of single Cy3–DOPE molecules on the NRK cell surface recorded at the video rate (30 frames/s) for a period of 5 s (150 frames). Their diffusion rates, D_{3s} (3-s time window), were 0.48 and 0.32 $\mu m^2/s$ (trajectories on the left and right, respectively). Movement of single molecules of Cy3–DOPE in LUV could not be imaged at the video rate because their diffusion is very fast. However, movement of DOPE molecules could be imaged when they were tagged with colloidal gold particles and the time resolution was enhanced to 25 μs (Fig. 2 B; Table I). The diffusion rate of Cy3–DOPE in the NRK cell membrane was smaller by a factor of ~20 than that of gold-tagged DOPE in LUV bilayers (Table I). (B) Histograms showing the distributions of the diffusion coefficients of DOPE in the NRK cell membrane. The arrowheads indicate the mean values. Shaded bars, D_{3s} (3-s time window) obtained by Cy3–DOPE at the video rate; open bars, $D_{100\mu s}$ (100-μs time window) obtained by gold-tagged DOPE at a 25-μs resolution (Fig. 2).

Downloaded from http://rupress.org/jcb/article-pdf/157/6/1071/1304489/jcb157761071.pdf by guest on 28 September 2022

Table I. **Parameters that characterize hop diffusion of DOPE at 25-μs and 2-ms time resolutions**

	Motional mode	Confinement size (median)					
Time resolution	**Hop + confined**	**Diameter**	**Area**	D_{micro}	D_{MACRO}	**Residency time**	**N[a]**
	%	nm	μm^2	$\mu m^2/s$	$\mu m^2/s$	ms	
Cell membrane							
25 μs	85	230	0.043	5.4	0.99	11	90
2 ms	94	750	0.44	1.6	0.17	650	84
LUV							
25 μs	6	NA[b]	NA	9.4	9.5	NA	18
Membrane bleb							
25 μs	44	NA	NA	8.8	7.4	NA	54
Membrane bleb + latrunculin-A							
25 μs	10	NA	NA	8.9	8.9	NA	30
Transferrin receptor							
25 μs	94	260	0.054	5.2	0.31	55	107
33 ms	83	710	0.4	0.210	0.070	1,800	70

Quantitative analysis is based on the method described previously (Powles et al., 1992; Kusumi et al., 1993; Sako and Kusumi, 1994; Tomishige et al., 1998). The diameter (L) of a compartment was determined as $(LxLy)1/2$, where Lx and Ly are the lengths of the confinement area in the x and y directions, respectively. The area was determined as $A = (\pi/4)LxLy$ (area of an ellipse whose major and minor axes are Lx and Ly, respectively). D_{micro} represents 100-ms and 20-ms scale diffusion rates (mean), whereas D_{MACRO} represents 50-ms (33-ms for LUV and membrane bleb) and 5-s scale diffusion rates (mean) for 25-ms and 2-ms time resolutions, respectively. The mean residency time within each compartment was determined as $A/4D_{MACRO}$.

[a]Number of particles.

[b]Not applicable or the actual number of particles observed is too small to be statistically significant. In the case of "membrane bleb," the variations are too large to obtain meaningful mean or median values.

warranting the use of single gold particle tracking to study DOPE movement in a time window of <100 ms.

Phospholipids undergo hop diffusion

Fig. 2 A shows two representative trajectories of DOPE at a time resolution of 25 μs obtained for a period of 56 ms. Statistical classification of such trajectories based on the mean square displacement plotted against time (MSD–t plot) was performed for each trajectory (Kusumi et al., 1993). As shown in Table I, 85% of DOPE molecules were found to undergo hop or confined-type diffusion. They were further analyzed based on the theory developed by Powles et al. (1992), which provided hop parameters, compartment size (L), residency time within a compartment, the microscopic

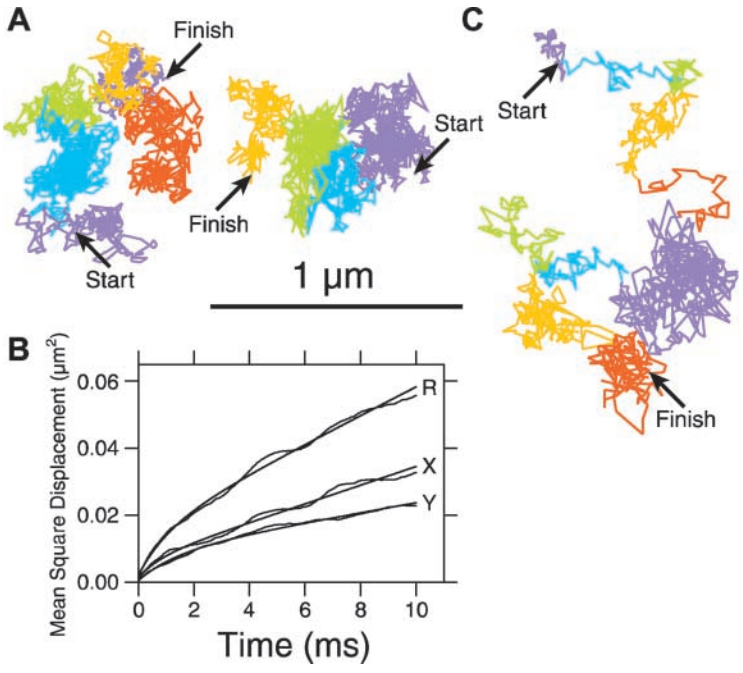

Figure 2. **Phospholipids undergo hop diffusion.** (A) Two representative trajectories of DOPE molecules recorded at a time resolution of 25 μs (40,500 frames/s) for a period of 56 ms (2,250 frames). A statistical analysis (Kusumi et al., 1993) indicated that these trajectories are not at all likely to be due to simple Brownian diffusion, and they were further subjected to quantitative hop analysis (Powles et al., 1992). Based on the number of compartments in each trajectory as estimated by the hop analysis (six and four compartments, 290 nm and 230 nm in diameter on average; D_{micro} = 6.5 and 4.6 $\mu m^2/s$ and D_{MACRO} = 1.9 and 1.2 $\mu m^2/s$, for the trajectories on the left and right, respectively), plausible compartments were identified by software developed to identify these corralling compartments, and are shown in different colors. For example, the left DOPE molecule moves in the following color-coded compartments: purple, blue, green, orange, red, and back to the previously orange-colored compartment (now shown in purple). Color coding is always in this sequence in this paper (Video 2 available at http://www.jcb.org/cgi/content/full/jcb.200202050/DC1). (B) An MSD–t plot for the trajectory on the right in A. It was fitted to a theoretical curve representing hop diffusion (Powles et al., 1992). The fit parameters include L, D_{micro}, and D_{MACRO}, and the residency time can be calculated from L and D_{MACRO}. X, Y, and R indicate diffusion in x and y directions and in a two-dimensional plane, respectively. (C) A typical trajectory of a DOPE molecule in an LUV bilayer, consisting of egg phosphatidylcholine/bovine brain phosphatidylserine/fluorescein–DOPE in a ratio of 500:50:1 by weight, recorded at a time resolution of 25 μs for a period of 33 ms (1,350 frames). A statistical analysis classified this trajectory into a simple Brownian mode. By way of comparison, fake compartments were assigned and indicated by different colors, based on visual examination. The prominent difference in appearance of the trajectories between A and C is that, in the case of real hop diffusion, adjacent compartments tend to be closely apposed and the trajectories are denser within a given compartment (Video 3).

Downloaded from http://rupress.org/jcb/article-pdf/157/6/1071/1304489/jcb157761071.pdf by guest on 28 September 2022

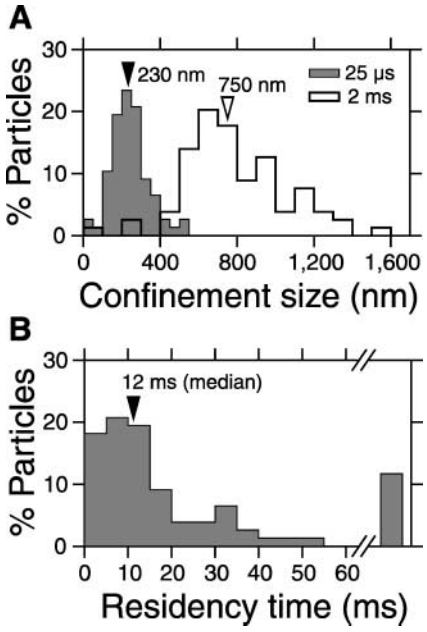

Figure 3. **DOPE is confined in 230-nm compartments and hops once every 12 ms (medians).** Distributions of the confinement size (A) and the residency time within 230-nm compartments (B) observed for DOPE hop diffusion. The arrowheads indicate the median values. (A) Shaded bars, 25-μs resolution; $n = 77$. Open bars, 2-ms resolution; $n = 79$. (B) The distribution of the residency time in 230-nm compartments observed at a 25-μs resolution. Note that the mean value is 11 ms as listed in Table I.

diffusion coefficient within a compartment (D_{micro}), and the macroscopic diffusion coefficient over many compartments (D_{MACRO}) as listed in Table I. The MSD–t plot for the trajectory on the right in Fig. 2 A and its fit to a theoretical curve for hop-type diffusion (Powles et al., 1992) are shown in Fig. 2 B. Such statistical and quantitative analyses found that the trajectories shown in Fig. 2 A consist of six (left) and four (right) apposing compartments. Individual plausible compartments were identified by software (as well as visual examination) developed to identify these confining compartments and are color coded in Fig. 2 A. Fig. 3 A shows the distribution of the confinement size. Its median value was 230 nm (Table I). The mean residency time within each 230-nm compartment was 11 ms (Table I; Fig. 3 B). Namely, DOPE molecules diffuse rapidly, but are confined within ~230-nm-ϕ compartments before hopping to adjacent compartments, such hopping occurring once an average of every ~11 ms. In this manner, DOPE undergoes long-range diffusion, a process we call "hop diffusion" (Kusumi et al., 1993; Sako and Kusumi, 1994; Kusumi and Sako, 1996; Tomishige et al., 1998; Tomishige and Kusumi, 1999; Video 2).

As a control, movement of DOPE molecules in the bilayers of large unilamellar vesicles (LUVs) was observed (Fig. 2 C; Video 3). Almost all (94%) the trajectories in LUVs were categorized into the simple Brownian mode. $D_{100\mu s}$ (100-μs time window) in the LUV membrane was 9.4 $\mu m^2/s$ on average (Table I), whereas $D_{100\mu s}$ within 230-nm compartments was 5.4 $\mu m^2/s$ on average (Table I; Fig. 1 B), which is comparable to $D_{100\mu s}$ in the LUV membrane. These results indicate that the diffusion inside a 230-nm compartment in the cell membrane is almost as fast as that of freely diffusing DOPE molecules in LUVs. It is thus concluded that lipid diffusion in the cell membrane is retarded not because the diffusion per se is slow, but dominantly because the cell membrane is compartmentalized with regard to lipid translational diffusion.

As described above, $D_{100\mu s}$ within the compartment (5.4 $\mu m^2/s$) is 40% smaller than that in LUVs (9.4 $\mu m^2/s$). This can be explained by the fact that the 100-μs time window is still too long to evaluate the correct diffusion rate within 230-nm compartments. DOPE is estimated to diffuse ~60

Table II. **Changes of phospholipid diffusion after trypsin treatment, partial cholesterol depletion, or partial depolymerization/stabilization of f-actin**

Time resolution	Treatment	Motional mode	Confinement size (median)		Residency time	N[a]
		Hop + confined	Diameter	Area		
		%	nm	μm^2	ms	
25 μs						
	Control	85	230	0.043	11	90
	Trypsin	88	250	0.049	16	33
	MβCD	96	280	0.061	13	28
	Latrunculin-A	97	340	0.093	20	32
	Jasplakinolide	96	240	0.044	23	29
2 ms						
	Control	94	750	0.44	650	84
	Trypsin	86	730	0.42	600	28
	MβCD	77[b]	860	0.58	600	60
	Latrunculin-A	85	1,100	0.90	740	124
	Jasplakinolide	90	670	0.36	1,100	96

Parameters that characterize hop diffusion of DOPE molecules. Cells were treated with trypsin to partially remove the pericellular matrix (61% of the extracellular proteins including extracellular domains of transmembrane proteins and extracellular matrix proteins, and 83% of heparan sulfate glycosaminoglycan), 4 mM methyl-β-cyclodextrin (MβCD) at 37°C for 30 min to partially deplete cholesterol, 50 nM latrunculin-A (f-actin depolymerizing drug), or 400 nM jasplakinolide (f-actin stabilizing drug) at 37°C for 5 min.

[a]Number of particles.

[b]The apparent low value here is probably due to a combination of a statistical error and the MβCD-induced slight spread of cells, which increased the compartment size by ~15% on average. The latter would make the diffusion of some DOPE molecules look more like simple Brownian.

Downloaded from http://rupress.org/jcb/article-pdf/157/6/1071/1304489/jcb157761071.pdf by guest on 28 September 2022

nm in 100 μs assuming a diffusion rate of 9.4 $\mu m^2/s$ ([4 × 9.4 $\mu m^2/s \times 10^{-4}$ s]$^{1/2}$), which indicates that even at the highest frame rates, the molecule will frequently rebound from a compartment wall during a frame and hence the displacement will be frequently underestimated.

The actin-based membrane skeleton, rather than the extracellular matrix or rafts, is responsible for compartmentalization of the cell membrane

How are the phospholipid molecules temporarily confined in these compartments? To investigate the possible involvement of extracellular domains of transmembrane proteins and the extracellular matrix due to the interaction with the attached gold particles, the cells were mildly treated with trypsin. Under the conditions in which 61% of the extracellular proteins (including extracellular domains of membrane proteins and extracellular matrix proteins) was cleaved off and 83% of heparan sulfate glycosaminoglycan was removed, the movement of DOPE molecules observed at a 25-μs resolution was not affected (Table II). Taken together with the fact that D_{100ms} is the same for both Cy3–DOPE and gold-tagged DOPE, it is concluded that the extracellular matrix and the extracellular domains of membrane proteins are not involved in the temporary corralling of phospholipids in 230-nm compartments.

Because DOPE, an unsaturated phospholipid, is excluded from cholesterol-enriched raft domains, the rafts may act as the diffusion obstacles for DOPE in the cell membrane. Therefore, we examined the effect of partial cholesterol depletion on DOPE diffusion (Kilsdonk et al., 1995). The effect of cholesterol depletion was minimal. The diffusion rate in 230-nm compartments was slightly increased (5.4 $\mu m^2/s$ to 7.1 $\mu m^2/s$), whereas no significant change was observed in other hop parameters (Table II). This result indicates that temporal corralling of DOPE is not caused by the exclusion from cholesterol-enriched raft domains.

After latrunculin-A treatment under conditions that partially depolymerize filamentous actin (Ayscough, 1998), greater compartments appeared for DOPE, the median diameter of 230-nm compartments increasing by a factor of ~1.5 (230 nm to 340 nm), or the area by a factor of ~2 (Table II; Fig. 4, left). Treatment with jasplakinolide, which stabilizes f-actin (Bubb et al., 2000), did not change the confinement size, but it increased the residency time by a factor of ~2 (11 ms to 23 ms) (Table II; Fig. 4, left), indicating that the compartment boundaries were stabilized. These results indicate that the movement of phospholipids in the outer leaf of the membrane, in spite of the lack of direct coupling with the membrane skeleton, can be regulated by the actin-based membrane skeleton fence structure.

Further, we compared DOPE movement with the movement of transferrin receptor (TfR), a transmembrane protein. We have previously shown that the cell membrane of the NRK cell is compartmentalized with regard to lateral diffusion of transmembrane proteins due to the interaction of their cytoplasmic domains with the actin-based membrane skeleton fence structure (Kusumi et al., 1993; Sako and Kusumi, 1994, 1995; Kusumi and Sako, 1996; Tomishige et al., 1998; Tomishige and Kusumi, 1999). As shown

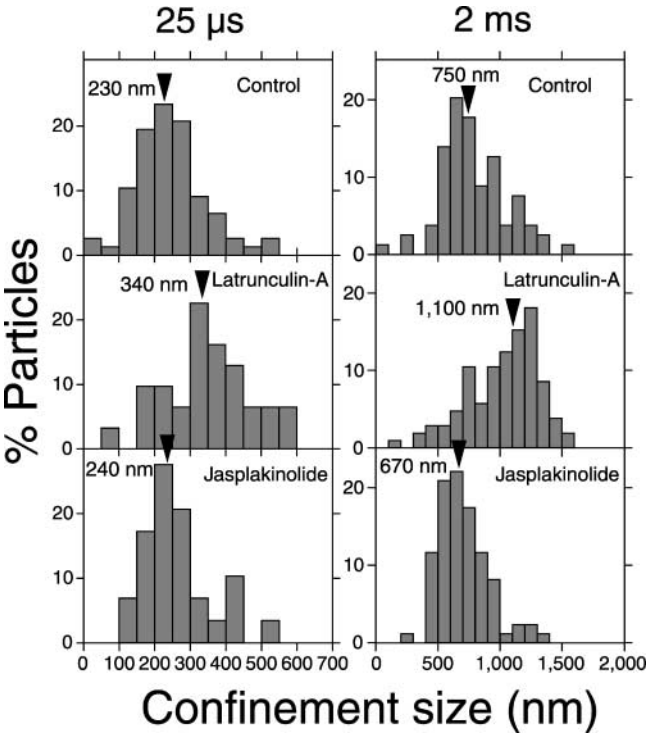

Figure 4. **Partial depolymerization of actin-based membrane skeleton increased the compartment sizes.** Arrowheads indicate the median values.

in Table I, we found that TfR also undergoes hop diffusion over compartments of 260 nm on average, which is about the same size as the compartments detected by DOPE (230 nm). Sako and Kusumi (1994) previously showed that the movement of TfR was confined in 700-nm compartments as observed at the video rate, a discrepancy we will come back to later in this paper.

As well, the movement of DOPE molecules was observed in membrane blebs, in which the membrane skeleton is partially depleted (Malorni et al., 1991). Approximately 60% (as compared with 15% in the control cell membrane) showed simple Brownian diffusion, and after latrunculin-A treatment, almost all (90%) trajectories observed in blebs were classified into the simple Brownian mode (Table I). Both $D_{100\mu s}$ and D_{33ms} were the same (8.9 $\mu m^2/s$), consistent with the classification into the simple Brownian mode. In addition, this rate is as fast as that in LUVs (9.4 $\mu m^2/s$). All these results indicate that the membrane skeleton is responsible for the hop diffusion of DOPE.

Anchored-protein picket model

This result is surprising because the phospholipid molecules we observed are localized in the outer leaf of the membrane, whereas the membrane skeleton is located on the cytoplasmic surface of the membrane. Meanwhile, as much as 30% of various kinds of transmembrane protein molecules are immobilized on the membrane skeleton meshwork (Ryan et al., 1988; Saxton, 1996). Furthermore, it has been proposed that immobilized transmembrane proteins significantly reduce the diffusion rate of membrane molecules (Jacobson et al., 1981) due to the circum-

Downloaded from http://rupress.org/jcb/article-pdf/157/6/1071/1304489/jcb15761071.pdf by guest on 28 September 2022

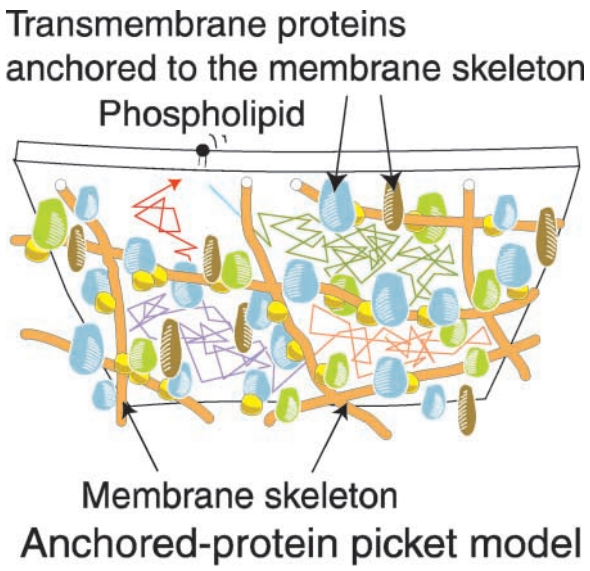

Figure 5. **Anchored membrane-protein picket model.** The transmembrane proteins anchored to the actin membrane skeleton meshwork effectively act as rows of pickets, and temporarily confine the movement of phospholipids through steric hindrance and circumferential slowing (packing or frictional) effects (Jacobson et al., 1981; Sperotto and Mouritsen, 1991; Almeida et al., 1992; Saxton, 1994; Bussell et al., 1995; Dodd et al., 1995). Our Monte Carlo simulations indicate that mobile particles cannot form effective diffusion barriers or obstacles.

ferential slowing effect referred to as the increased packing near the protein (in terms of the free volume theory) (Sperotto and Mouritsen, 1991; Almeida et al., 1992), or to the increased hydrodynamic friction (in terms of the hydrodynamic theory) (Bussell et al., 1995; Dodd et al., 1995). In light of the proceeding, we propose an anchored membrane-protein picket model (Fig. 5) in which transmembrane proteins anchored to the actin-based membrane skeleton effectively act as pickets along the membrane skeleton fence. Such rows of pickets possibly confine the movement of phospholipids through both steric hindrance (Saxton, 1994) and circumferential slowing. A major characteristic of this model is the coupling of the membrane skeleton to lipids in the outer leaflet of the membrane by means of the membrane skeleton–anchored proteins.

To test this model, a series of Monte Carlo simulations of the diffusion of phospholipids, including the effects of steric hindrance and circumferential slowing caused by proteins anchored to the membrane skeleton, were performed. The free area theory of lipid diffusion gives an expression for the reduction in the diffusion constant that extends radially from the immobilized proteins (Almeida et al., 1992). Fig. 6 A displays typical Monte Carlo trajectories. To reproduce experimental parameters such as the residency time of DOPE within a compartment (11 ms), ~16, 24, and 34% coverage of the compartment boundaries by 1-, 2-, and 3-nm protein obstacles was required, respectively (Fig. 6 B).

The NRK cell membrane is doubly compartmentalized

A representative long-term 2-s trajectory (compared with the short-term 56-ms trajectories displayed in Fig. 2 A) of a DOPE

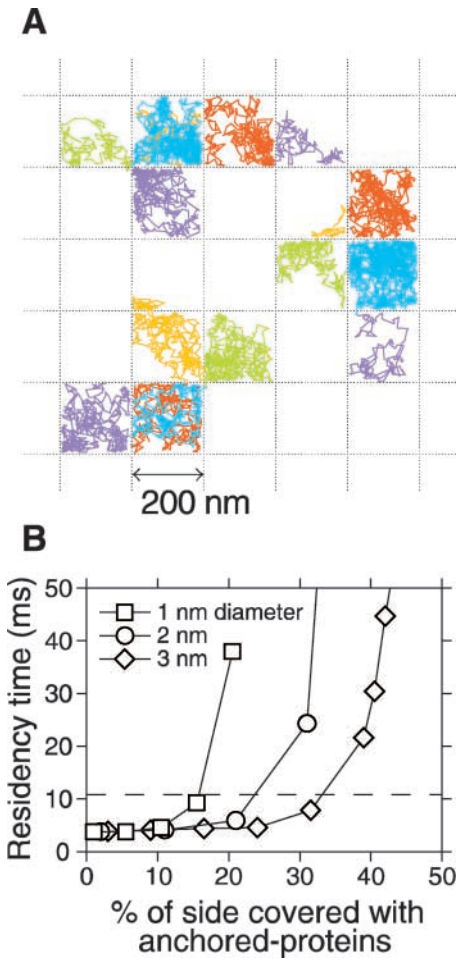

Figure 6. **A series of Monte Carlo simulations support the anchored-protein picket model.** (A) Typical trajectories of test particles (2,250 steps with 25-μs intervals) bounded by immobile obstacles as observed in Monte Carlo simulations. Stationary barrier obstacles of set hard-core radius were placed along the edges of a square grid (200 nm × 200 nm) such that there were a set number of barriers per unit cell. The effects of steric hindrance and circumferential slowing due to anchored proteins are included. (B) Plot of residency time versus percent of the side of the compartment boundary covered with anchored membrane proteins (1, 2, or 3 nm in diameter). 100 trajectories were generated and the mean D_{50ms} (50-ms time window) was obtained for each condition. The mean residency time was determined as $(200\ \text{nm})^2/4D_{50ms}$. The dashed line shows the experimentally determined 11-ms residency time for 230-nm compartments. About 16, 24, and 34% coverage of the boundary (31, 24, and 23 protein molecules on a given 200-nm barrier) with 1-, 2-, and 3-nm-ϕ anchored proteins, respectively, was required to obtain the residency time similar to the experimental value.

molecule obtained at a 25-μs resolution is shown in Fig. 7 A, left, indicating the presence of compartments greater than the 230-nm compartments. Typical smaller 230-nm compartments present within the greater purple compartment are shown by circles in Fig. 7 A, left (enlarged in Fig. 7 C). Instances of hops between greater compartments at 0.5–1-s intervals are apparent when the locations of gold–DOPE complexes at 81-frame intervals were connected by straight lines (like a time-lapse trajectory at a time resolution of 2 ms) as shown in Fig. 7 A, right. These results clearly indicate the double compartmentalization of the NRK cell membrane (Fig. 8).

Downloaded from http://rupress.org/jcb/article-pdf/157/6/1071/1304489/jcb15761071.pdf by guest on 28 September 2022

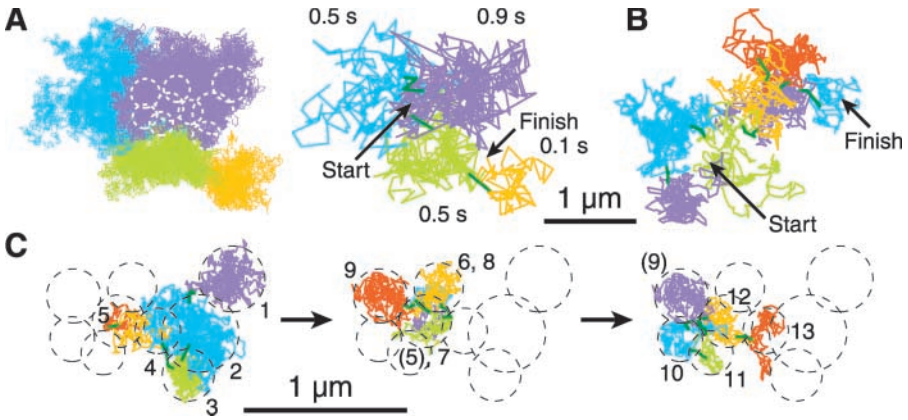

Figure 7. **NRK cell membrane is doubly compartmentalized with regard to translational diffusion of phospholipids.** (A, left) A typical long-term trajectory of DOPE recorded at 25-μs resolution for a period of 2 s (81,000 frames). (A, right) A trajectory that sampled the coordinates of the left trajectory at 81-frame intervals, giving a time-lapse trajectory at a time resolution of 2 ms. Plausible compartments greater than 230-nm compartments were identified, and are shown in different colors with residency times: purple, 0.9 s; blue, 0.5 s; green, 0.5 s; orange, 0.1 s. The instances of intercompartmental hops are shown in dark green. (B) A representative trajectory of a DOPE molecule observed at a 2-ms time resolution for a period of 5 s (2,500 frames). The particle started from the purple compartment at the left-bottom, and after it reached the orange compartment, it hopped to the red compartment and came back to the orange compartment (shown in purple), which appeared to have shifted slightly toward the right. Finally, the molecule hopped to the blue compartment. The instances of intercompartmental hops are shown in dark green. (Video 4). (C) Intercompartmental hops among 230-nm subcompartments for a period of 120 ms. Individual compartments are color coded and numbered sequentially. The circles coincide with those in the purple (750 nm) compartment in A (left). Note that compartments 5, 7, and 12 (also 6 and 8; 4 and 13) match with regard to their positions. The instances of intercompartmental hops are shown in dark green.

Because the quantitative analysis for the doubly compartmentalized movement is overly complicated, recordings at the time resolution of 2 ms (a spatial precision of 6.9 nm at this recording rate) were performed to characterize the greater compartments. The hops among 230-nm compartments, which take place an average of once every 11 ms, are not detected due to the sparsity of points generated at the 2-ms resolution.

Fig. 7 B shows a representative trajectory of a DOPE molecule recorded at a time resolution of 2 ms for a period of 5 s (Video 4). The statistical analysis categorized 94% of DOPE movements into hop or confined-type diffusion (Table I) at this time resolution. The quantitative hop analysis provided the distribution of the confinement size (Fig. 3 A), its median value being 750 nm. The mean residency time within each 750-nm compartment was 0.65 s (Table I). Plausible compartments in the trajectory in Fig. 7 B were identified by a computer program developed here (the same as used for Fig. 2 A) and are shown in different colors. Long-range diffusion occurs by successive hops among 750-nm compartments.

The residency time of DOPE in 750-nm compartments can be estimated from D_{3s} for Cy3–DOPE (0.42 $\mu m^2/s$) and the average compartment size determined with gold-tagged DOPE (750 nm). The D_{3s} for Cy3–DOPE is likely to give more correct D_{3s} than that for gold-tagged DOPE because the D_{3s} obtained with gold probes is smaller than D_{3s} for Cy3–DOPE by a factor of 2.5, as stated in the beginning of the Results, possibly due to moderate steric or cross-linking effects of gold particles on long-range diffusion. Meanwhile, the compartment size could only be determined with gold-tagged DOPE, and the size is likely to be the same for both Cy3–DOPE and gold-tagged DOPE. Therefore, the residency time of Cy3–DOPE in 750-nm compartments is estimated to be 0.33 s ($[0.75\ \mu m]^2/[4 \times 0.42\ \mu m^2/s]$) on average.

The diffusion rate inside 750-nm compartments (D_{20ms}) is 1.6 $\mu m^2/s$ (Table I), which coincides with the diffusion rate expected from a series of intercompartmental hops over 230-nm compartments once every 11 ms ($[0.23\ \mu m]^2/[4 \times 11\ ms] = 1.2\ \mu m^2/s$) (see the model in Fig. 8). In addition to the reduction of the diffusion rate from 5.4 $\mu m^2/s$ to 1.6 $\mu m^2/s$ due to the confinement by 230-nm compartments, the further reduction in the diffusion rate by a factor of 4 to 0.42 $\mu m^2/s$ (D_{3s} for Cy3–DOPE) is consistent with the presence of barriers every 750 nm. These results support the model in which the NRK cell membrane is compartmentalized into 750-nm and then into 230-nm compartments with regard to the lateral diffusion of DOPE molecules (Fig. 8).

The presence of such double compartments is not likely to be an artifact of observing 230-nm compartments at lower time resolutions, because the distinct 230- and 750-nm com-

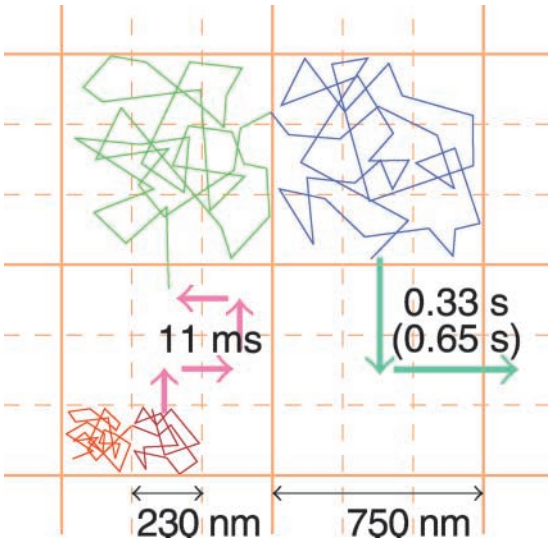

Figure 8. **A model of double compartmentalization for DOPE diffusion.** A DOPE molecule undergoes free diffusion inside a 230-nm compartment for an average of 11 ms, and then hops to an adjacent compartment. It also experiences confinement in the greater 750-nm compartments. The diffusion rate within a 750-nm compartment reflects the rate of hops among 230-nm compartments. The residency time within the 750-nm compartment is 0.33 s on average, which is ~30 times longer than that for a 230-nm compartment. This residency time was estimated from the macroscopic diffusion rate of Cy3–DOPE.

Downloaded from http://rupress.org/jcb/article-pdf/157/6/1071/1304489/jcb157761071.pdf by guest on 28 September 2022

partments are seen in 25-μs observations (Fig. 7, A and C), and although we found compartmentalized diffusion of DOPE in other cell types, such as CHO, PtK2, COS1, and ECV304 cells, these cells did not show any signs of double compartmentalization. Therefore, double compartmentalization must be characteristic of the NRK cell membrane. Further quantitative analysis to confirm double compartmentalization is given in the online supplemental materials (available at http://www.jcb.org/cgi/content/full/jcb.200202050/DC1).

Double compartmentalization for TfR diffusion in the NRK cell membrane

As shown in Table I, TfR diffusion was also found to be doubly compartmentalized into 710-nm compartments and then into 260-nm compartments. This is consistent with double compartmentalization of DOPE molecules into 750- and 230-nm compartments, suggesting the involvement of the membrane skeleton for the greater compartment.

Previously, Sako and Kusumi (1994, 1995) demonstrated the existence of 700-nm compartments with regard to the diffusion of TfR in NRK cells. However, in these previous studies performed at a video rate time resolution (33 ms), the smaller 260-nm compartments were not observed. Because TfR hops among 260-nm compartments an average of once every 55 ms (Table I), there was no way of detecting the smaller compartments at this frame rate of every 33 ms. The problem of the unexpectedly slow diffusion rate within 700-nm compartments found previously (~0.1 $\mu m^2/s$) (Kusumi et al., 1993; Sako and Kusumi, 1994) is clarified in the present investigation: namely, TfR diffusion in 700-nm compartments is slowed due to the presence of smaller 260-nm compartments within them.

The next question, then, is whether there are yet smaller compartments within 260-nm compartments (i.e., triple compartmentalization). We think it very unlikely because the diffusion rate of TfR within a 260-nm compartment is almost as great as that of DOPE in LUVs or in bleb membranes (reduction by ~40% can be explained by the reflection of TfR molecules at the boundary and the lack of time resolution for its visualization, the same argument used to explain the reduction of $D_{100\mu s}$ for gold-tagged DOPE). The hop rate for TfR over 700-nm compartments is once every 1.8 s on average, which is ~10 times faster than that reported previously (Sako and Kusumi, 1994). This is probably due to better control of preparation of gold probes to avoid cross-linking in this study.

The agreement of sizes of both greater and smaller compartments for DOPE and TfR again suggests that the membrane skeleton is involved in the formation of compartments of both sizes.

Anchored-protein pickets also form the boundaries of greater compartments

We examined again the involvement of the extracellular matrix, extracellular domains of membrane proteins, cholesterol-enriched rafts, and actin-based membrane skeleton in DOPE hop diffusion over 750-nm compartments observed at a 2-ms time resolution, as was done for 230-nm compartments. Neither trypsin treatment nor cholesterol depletion caused any significant change in DOPE's hop movement over 750-nm compartments (Table II, bottom part indicated by "2 ms," but see footnote b). However, partial depolymerization of f-actin with latrunculin-A increased the median diameter of 750-nm compartments by a factor of ~1.5 (750 nm to 1,100 nm), or the area by a factor of ~2. Meanwhile, stabilization with jasplakinolide increased the residency time by a factor of ~2 (650 ms to 1,100 ms) (Table II, bottom; Fig. 4, right; Video 5). These results indicate that pickets located along the actin membrane skeleton fence are again responsible for the corralling of DOPE molecules inside 750-nm compartments.

Discussion

We have shown, for the first time, that the cell membrane is compartmentalized with regard to lateral diffusion of phospholipids, and thus their long-range diffusion is largely limited by the hop rate across the compartment boundaries. Three types of experimental results indicated that the actin-based membrane skeleton is involved in such compartmentalization. (1) The boundaries are not dependent on the extracellular matrix, extracellular domains of the membrane proteins, or cholesterol content in the membrane, but are modulated by modification of the actin-based membrane skeleton. (2) DOPE undergoes rapid simple Brownian diffusion, rather than hop diffusion, in membrane blebs in which the membrane skeleton is largely depleted. (3) The compartment size for phospholipids is almost identical to that found for TfR, whose compartment size is largely determined by the membrane skeleton fence. Based on these results, together with the previous findings of membrane skeleton fences for transmembrane proteins (Kusumi et al., 1993; Sako and Kusumi, 1994, 1995; Kusumi and Sako, 1996; Tomishige et al., 1998; Tomishige and Kusumi, 1999), we propose here an "anchored membrane-protein picket model." In this model, transmembrane proteins anchored to the membrane skeleton are called "pickets," as they act as posts along the membrane skeleton fence. These rows of pickets act as effective diffusion barriers due to steric hindrance as well as circumferential slowing (packing and frictional) effects even for phospholipids in the outer leaf of the membrane.

These immobilized picket proteins are likely to include various transmembrane proteins, rather than limited protein species, as we have found that almost all transmembrane proteins we have studied so far exhibited various amounts of immobilized populations (even after excluding the populations in the process of internalization; Kusumi and Sako, 1996). In addition, transmembrane proteins transiently associated with the membrane skeleton also act as diffusion barriers if they are immobilized longer than the period in which phospholipids are within the boundary regions (estimated to be ~100 μs, assuming that the boundary region is ~20 nm wide and the effective diffusion coefficient of phospholipid is decreased to 1 $\mu m^2/s$ in this region; $[0.02\ \mu m]^2/[4 \times 1\ \mu m^2/s] = 100\ \mu s$).

Our earlier work on transmembrane protein diffusion led us to propose the membrane skeleton fence model, in which the cytoplasmic domains of transmembrane proteins collide with the membrane skeleton, which induces temporary confinement (corralling). A transmembrane protein could hop from a compartment to an adjacent one when the membrane skeleton fluctuates to allow space between itself and the membrane, when the membrane skeleton is transiently dissociated, or

Downloaded from http://rupress.org/jcb/article-pdf/157/6/1071/1304489/jcb15761071.pdf by guest on 28 September 2022

when the transmembrane protein has reached the boundary while possessing sufficient kinetic energy to surmount the barrier potential. The anchored-protein pickets found in the present study would provide another diffusion barrier for transmembrane proteins in the cell membrane. Because the picket barriers would act on all membrane molecules, both the membrane skeleton fence and the anchored-protein pickets would limit movement of transmembrane proteins. Because these interactions are found in all cell types (such as CHO, PtK2, COS1, and ECV304) we have observed so far (unpublished data), they are likely to be universal in the reduction of the diffusion rates. Double compartmentalization has been found only in NRK cells among the cells we have studied thus far. The compartment sizes of the NRK cell membrane (230 and 750 nm for DOPE; 260 and 710 nm for TfR) are substantially greater than others (unpublished data), which we suspect might make it necessary for NRK cells to possess a more stable membrane skeleton every ~700 nm on average.

There is growing interest in the size of rafts that may range from a scale of several tens to several hundreds of nanometers (for reviews see Jacobson and Dietrich, 1999; Edidin, 2001). Pralle et al. (2000) and Varma and Mayor (1998) found that the size may be ~50–70 nm in diameter, whereas others suggested that stabilized raft may reach a diameter of a few hundred nanometers to nearly a micrometer (Sheets et al., 1997; Simson et al., 1998; Schütz et al., 2000; Dietrich et al., 2002). Compartmentalization of lipid diffusion in the cell membrane due to anchored-protein pickets on the actin-based membrane skeleton would provide an important basis for understanding how the diffusion data relate to raft size and lifetime. Different conclusions regarding the properties of rafts in different biological contexts may be explained based on the notion of the compartmentalized cell membrane even for phospholipids (the present study) and glycosylphosphatidylinositol-linked proteins (unpublished data).

The picket barrier, which affects the movement of even lipid molecules in the outer leaf, could play a major role in dramatically reducing the diffusion of both transmembrane and glycosylphosphatidylinositol-linked receptor molecules upon oligomerization and/or partitioning into stabilized signaling rafts. As soon as signaling molecule complexes, such as dimerized (activated) receptors, receptors bound by the cytoplasmic signaling molecules, and clustering-induced stable rafts, are formed, the pickets within the cell membrane, coupled with a corralling effect of the membrane skeleton fence on the cytoplasmic surface, would cause the immediate arrest of these molecular complexes within the membrane compartments where extracellular signals were received ("oligomerization-induced trapping;" Iino et al., 2001). Therefore, the anchored membrane-protein picket barriers would play a critical role in localizing intracellular signaling molecules and thereby "memorizing" where extracellular signals were received, an occurrence that may be required for polarized responses of cells, such as chemotaxis, cytoskeletal reorganization, and protrusion of processes.

Materials and methods

Cell culture

NRK fibroblastic cells were grown in Ham's F12 medium supplemented with antibiotics and 10% FBS. Cells were plated on 12-mm-ϕ coverslip-based dishes (for single fluorophore imaging) or 18-mm × 18-mm coverslips (for high-speed video imaging) and used 2 d later.

Lipid probe incorporation

DOPE was purchased from Avanti Polar Lipids, Inc., Cy3 from Amersham Pharmacia Biotech, and FITC (isomer I) from Molecular Probes Inc. For single fluorophore imaging, DOPE conjugated with Cy3 in the head group region (Cy3–DOPE) was dissolved in 10 μl of methanol (10 μg/ml), which was then diluted to 1 ml with HBSS buffered with 2 mM Pipes, pH 7.2, (HP) while vortexing vigorously. It was further diluted to 0.4 ng/ml for the appropriate incorporation into cells at 37°C. Individual Cy3–DOPE molecules were observed on the dorsal cell membrane at the video rate using an objective-type total internal reflection microscope (Sako et al., 2000; Iino et al., 2001). For high-speed video imaging, DOPE conjugated with fluorescein in the head group region was diluted with the HP medium in the same way as Cy3–DOPE except that the final concentration of fluorescein–DOPE was 2 μg/ml.

Gold probe preparation and labeling

40-nm-ϕ colloidal gold particles (BBInternational) conjugated with Fab fragments of antifluorescein antibodies (Molecular Probes Inc.) were prepared by mixing 50 μl of 13.2 μg/ml Fab in 2 mM phosphate buffer, pH 7.2, and 500 μl of colloidal gold suspension (1.2 μg/ml of Fab in the mixture) (Tomishige et al., 1998). After incubating for 1 h at room temperature, the Fab–gold complex was further stabilized with 0.05% Carbowax 20 M (Sigma-Aldrich). After two washes by centrifugation and resuspension in 0.05% Carbowax/2 mM phosphate buffer, pH 7.2, the conjugates were resuspended in 0.05% Carbowax 20M/HBSS buffered with 2 mM Pipes, pH 7.2 (HP–CW). The gold probe suspension (~0.02 nM of gold particles) was added to cells that had been incubated with fluorescein–DOPE.

The amount of Fab fragments mixed with the gold particles was varied to minimize the effect of lipid cross-linking by the gold probe. As the Fab concentration was reduced (when it was mixed with gold particles), the diffusion rate of the gold–DOPE complex determined at the video rate (D_{100ms}) was increased, and it reached a plateau value of 0.49 $\mu m^2/s$ when 1.2 μg/ml of Fab was used. At this concentration, the ratio of particles bound specifically versus nonspecifically (without incorporation of fluorescein–DOPE) was 7.3 to 1 (13.2 vs. 1.8 particles/cell on average).

Colloidal gold particles conjugated with bovine holo transferrin (Wako) were prepared according to Sako and Kusumi (1994) while minimizing the effect of cross-linking by reducing the transferrin concentration mixed with the gold particles.

LUVs, as large as 10 μm in diameter, were prepared essentially according to Akashi et al. (1996) and attached to poly-L-lysine–coated coverslips.

Membrane blebs, up to 20 μm in diameter, were formed by incubating the cells with 1 mM menadione (Sigma-Aldrich) in the HP medium at 37°C for 1 h (Malorni et al., 1991). When further removal of the membrane skeleton was desired, the cells were then treated with latrunculin-A in the same way as described below.

High-speed video microscopy

High-speed video microscopy was performed as described previously (Tomishige et al., 1998). The precision of the position determination was estimated from the standard deviation of the coordinates of 40-nm-ϕ gold particles fixed in a 10% polyacrylamide gel on a poly-L-lysine–coated coverslip, and was 17 nm and 6.9 nm at time resolutions of 25 μs and 2 ms, respectively. On the cell membrane, the positions correspond to the probability distribution peaks of the diffusing gold particles during each exposure time. The quantitative analysis of lipid movement was performed based on the MSD methods described previously (Powles et al., 1992; Kusumi et al., 1993; Sako and Kusumi, 1994; Tomishige et al., 1998). For each trajectory of a particle, MSD, $<(\Delta r(\Delta t))^2>$, for every time interval was calculated according to the formula:

$$\mathrm{MSD}(n\delta t) = \frac{1}{N-1-n}\sum_{j=1}^{N-1-n}\{[x(j\delta t + n\delta t) - x(j\delta t)]^2 + [y(j\delta t + n\delta t) - y(j\delta t)]^2\} \quad (1)$$

(Qian et al., 1991; Kusumi et al., 1993), where δt is the time resolution and (x(jδt + nδt), y(jδt + nδt)) describes the particle position after a time interval $\Delta t_n = n\delta t$ after starting at position (x(jδt), y(jδt)), N is the total number of frames in the sequence, n and j are positive integers, and n determines the time increment.

Downloaded from http://rupress.org/jcb/article-pdf/157/6/1071/1304489/jcb15761071.pdf by guest on 28 September 2022

Tilting and reorientation of lipids are not likely to seriously affect the measurement of the lateral diffusion rate even at a 25-μs resolution because $D_{100\mu s}$ of DOPE in LUVs (9.4 $\mu m^2/s$; Table I) is almost the same as D_{33ms} (9.5 $\mu m^2/s$).

Treatment of cells with trypsin and drugs

To partially remove the extracellular domains of membrane proteins and the extracellular matrix, cells were treated with 25 μg/ml trypsin (Difco Laboratories) in the HP medium at 37°C for 10 min. To monitor the extent of cleavage, extracellular surface proteins were first tagged with sulfosuccinimidyl biotin (Sigma-Aldrich) and visualized by fluorescein–streptavidin (Molecular Probes Inc.) before and after trypsin digestion. Heparan sulfate glycosaminoglycan was detected by indirect immunofluorescence method using HepSS-1 antiheparan sulfate (Seikagaku Corp.) and fluorescein–goat anti–mouse antibody (Zymed Laboratories). Epifluorescence images of cells were quantitated by MetaView software (Universal Imaging Corp.). For cholesterol depletion (Kilsdonk et al., 1995), cells were incubated in the HP medium containing 4 mM methyl-β-cyclodextrin (Sigma-Aldrich) at 37°C for 30 min. Latrunculin-A and jasplakinolide were provided by G. Marriott (University of Wisconsin, Madison, WI). Cells were incubated in the HP–CW medium containing 50 nM latrunculin-A (Ayscough, 1998) or 400 nM jasplakinolide (Bubb et al., 2000) on the microscope stage at 37°C for 5 min. Microscopic observations were completed within 30 min after addition of drugs, before large morphological changes of the cells took place. Longer observations or higher concentrations of latrunculin-A and jasplakinolide caused the collapse and aggregation of the actin-based membrane skeleton, which results in the immobilization of gold probes, and hence were avoided.

Computer simulation

The two-dimensional, Brownian Monte Carlo algorithm employed here (Rossky et al., 1978) takes steps that are predicated on the Langevin equation, and hence allows the inclusion of the circumferential slowing effect. Extensions were made to include a spatially variable diffusivity as in Evans and Ritchie (1997). The variation in the diffusion coefficient away from the protein obstacles was taken from free area theory using the parameters of Almeida et al. (1992) (a coherence length of 15 Å for the free area disturbance, 0.25 for the relative critical free area next to an obstacle with respect to the bulk free area and a ratio of 2.5 for the relative critical free area for diffusion with respect to the bulk free area).

Online supplemental materials

Included in the online supplemental materials (available at http://www.jcb.org/cgi/content/full/jcb.200202050/DC1) are the quantitative analysis (Fig. S1) to confirm double compartmentalization of the NRK cell membrane, and the videos (Videos 1–5) showing movement of single DOPE molecules in the cell membrane, recorded by single fluorophore imaging and high-speed single particle imaging techniques. Video 1 shows the movement of single Cy3–DOPE molecules and a gold-tagged DOPE molecule on the NRK cell surface recorded at the video rate. Arrowheads in the first sequence indicate some of the DOPE molecules (with its fluorescence signal lasting longer than the average). Fluorescent spots are photobleached in single steps, indicating that these represent single Cy3–DOPE molecules. Video 2 shows the hop diffusion of gold-tagged DOPE over 230-nm compartments observed at a 25-μs resolution for 62 ms (×270 slowed). In the second sequence, their trajectories are superimposed. In the trajectories, plausible compartments are shown in different colors, based on quantitative analysis. 750-nm compartments cannot be detected in the 62-ms period. Video 3 shows the movement of gold-tagged DOPE (×270 slowed) diffusing freely on a large unilamellar vesicle, observed at a 25-μs resolution. In the second sequence, its trajectory is superimposed. Video 4 shows the hop diffusion of gold-tagged DOPE over 750-nm compartments, observed at a 2-ms resolution (×3.3 slowed). At this time resolution, the 230-nm compartments, where DOPE stays for 11 ms on average, cannot be identified due to the sparsity of points. Video 5 shows the effects of f-actin depolymerizing/stabilizing drugs on the movement of DOPE at a 2-ms resolution. Partial depolymerization of the actin-based membrane skeleton by latrunculin-A treatment increased the compartment size by a factor of ~2 in area, whereas stabilization by jasplakinolide increased the residency time by a factor of ~2.

We would like to thank G. Marriott for providing latrunculin-A and jasplakinolide, K. Metz-Honda (ERATO) for synthesizing Cy3–DOPE, R. Iino (ERATO) for building the total internal reflection microscope, and K. Suzuki (ERATO) and C. Dietrich (University of North Carolina, Chapel Hill, NC) for their helpful advice and discussion.

Submitted: 12 February 2002
Revised: 22 April 2002
Accepted: 23 April 2002

References

Akashi, K., H. Miyata, H. Itoh, and K. Kinosita, Jr. 1996. Preparation of giant liposomes in physiological conditions and their characterization under an optical microscope. *Biophys. J.* 71:3242–3250.

Almeida, P.F.F., W.L.C. Vaz, and T.E. Thompson. 1992. Lateral diffusion and percolation in two-phase, two-component lipid bilayers. Topology of the solid-phase domains in-plane and across the lipid bilayer. *Biochemistry.* 31: 7198–7210.

Ayscough, K. 1998. Use of latrunculin-A, an actin monomer-binding drug. *Methods Enzymol.* 298:18–25.

Bubb, M.R., I. Spector, B.B. Beyer, and K.M. Fosen. 2000. Effects of jasplakinolide on the kinetics of actin polymerization. An explanation for certain in vivo observations. *J. Biol. Chem.* 275:5163–5170.

Bussell, S.J., D.L. Koch, and D.A. Hammer. 1995. Effect of hydrodynamic interactions on the diffusion of integral membrane proteins: diffusion in plasma membranes. *Biophys. J.* 68:1836–1849.

Dietrich, C., B. Yang, T. Fujiwara, A. Kusumi, and K. Jacobson. 2002. Relationship of lipid rafts to transient confinement zones detected by single particle tracking. *Biophys. J.* 82:274–284.

Dodd, T.L., D.A. Hammer, A.S. Sangani, and D.L. Koch. 1995. Numerical simulations of the effect of hydrodynamic interactions on diffusivities of integral membrane proteins. *J. Fluid Mech.* 293:147–180.

Edidin, M. 2001. Shrinking patches and slippery rafts: scales of domains in the plasma membrane. *Trends Cell Biol.* 11:492–496.

Evans, E., and K. Ritchie. 1997. Dynamic strength of molecular adhesion bonds. *Biophys. J.* 72:1541–1555.

Iino, R., I. Koyama, and A. Kusumi. 2001. Single molecule imaging of green fluorescent proteins in living cells: E-cadherin forms oligomers on the cell surface. *Biophys. J.* 80:2667–2677.

Jacobson, K., Y. Hou, Z. Derzko, J. Wojcieszyn, and D. Organisciak. 1981. Lipid lateral diffusion in the surface membrane of cells and in multibilayers formed from plasma membrane lipids. *Biochemistry.* 20:5268–5275.

Jacobson, K., and C. Dietrich. 1999. Looking at lipid rafts? *Trends Cell Biol.* 9:87–91.

Kilsdonk, E.P., P.G. Yancey, G.W. Stoudt, F.W. Bangerter, W.J. Johnson, M.C. Phillips, and G.H. Rothblat. 1995. Cellular cholesterol efflux mediated by cyclodextrins. *J. Biol. Chem.* 270:17250–17256.

Kusumi, A., and Y. Sako. 1996. Cell surface organization by the membrane skeleton. *Curr. Opin. Cell Biol.* 8:566–574.

Kusumi, A., Y. Sako, and M. Yamamoto. 1993. Confined lateral diffusion of membrane receptors as studied by single particle tracking (nanovid microscopy). Effects of calcium-induced differentiation in cultured epithelial cells. *Biophys. J.* 65:2021–2040.

Ladha, S., A.R. Mackie, L.J. Harvey, D.C. Clark, E.J. Lea, M. Brullemans, and H. Duclohier. 1996. Lateral diffusion in planer lipid bilayers: a fluorescence recovery after photobleaching investigation of its modulation by lipid composition, cholesterol, or alamethicin content and divalent cations. *Biophys. J.* 71:1364–1373.

Lee, G.M., F. Zhang, A. Ishihara, C.L. McNeil, and K. Jacobson. 1993. Unconfined lateral diffusion and an estimate of pericellular matrix viscosity revealed by measuring the mobility of gold-tagged lipids. *J. Cell Biol.* 120:25–35.

Malorni, W., F. Iosi, F. Mirabelli, and G. Bellomo. 1991. Cytoskeleton as a target in menadione-induced oxidative stress in cultured mammalian cells: alterations underlying surface bleb formation. *Chem. Biol. Interact.* 80:217–236.

Pralle, A., P. Keller, E.L. Florin, K. Simons, and J.K.H. Hörber. 2000. Sphingolipid-cholesterol rafts diffuse as small entities in the plasma membrane of mammalian cells. *J. Cell Biol.* 148:997–1008.

Powles, J.G., M.J.D. Mallett, G. Rickayzen, and W.A.B. Evans. 1992. Exact analytic solutions for diffusion impeded by an infinite array of partially permeable barriers. *Proc. R. Soc. Lond. A.* 436:391–403.

Qian, H., M.P. Sheetz, and E.L. Elson. 1991. Single particle tracking. Analysis of diffusion and flow in two-dimensional systems. *Biophys. J.* 60:910–921.

Rossky, P.J., J.D. Doll, and H.L. Friedman. 1978. Brownian dynamics as smart Monte Carlo simulation. *J. Chem. Physiol.* 69:4628–4633.

Ryan, T.A., J. Myers, D. Holowka, B. Baird, and W.W. Webb. 1988. Molecular crowding on the cell surface. *Science.* 239:61–64.

Sako, Y., and A. Kusumi. 1994. Compartmentalized structure of the plasma membrane for receptor movements as revealed by a nanometer-level motion anal-

Downloaded from http://rupress.org/jcb/article-pdf/157/6/1071/1304489/jcb15761071.pdf by guest on 28 September 2022

ysis. *J. Cell Biol.* 125:1251–1264.

Sako, Y., and A. Kusumi. 1995. Barriers for lateral diffusion of transferrin receptor in the plasma membrane as characterized by receptor dragging by laser tweezers: fence versus tether. *J. Cell Biol.* 129:1559–1574.

Sako, Y., S. Minoguchi, and T. Yanagida. 2000. Single-molecule imaging of EGFR signaling on the surface of living cells. *Nat. Cell Biol.* 2:168–172.

Saxton, M.J. 1994. Anomalous diffusion due to obstacles: a Monte Carlo study. *Biophys. J.* 66:394–401.

Saxton, M.J. 1996. Anomalous diffusion due to binding: a Monte Carlo study. *Biophys. J.* 70:1250–1262.

Schütz, G.J., G. Kada, V.P. Pastushenko, and H. Schindler. 2000. Properties of lipid microdomains in a muscle cell membrane visualized by single molecule microscopy. *EMBO J.* 19:892–901.

Sheets, E.D., G.M. Lee, R. Simson, and K. Jacobson. 1997. Transient confinement of a glycosylphosphatidylinositol-anchored protein in the plasma membrane. *Biochemistry.* 36:12449–12458.

Simons, K., and D. Toomre. 2000. Lipid rafts and signal transduction. *Nat. Rev. Mol. Cell Biol.* 1:31–39.

Simson, R., B. Yang, S.E. Moore, P. Doherty, F.S. Walsh, and K.A. Jacobson. 1998. Structural mosaicism on the submicron scale in the plasma membrane. *Biophys. J.* 74:297–308.

Sonnleitner, A., G.J. Schütz, and T. Schmidt. 1999. Free Brownian motion of individual lipid molecules in biomembranes. *Biophys. J.* 77:2638–2642.

Sperotto, M.M., and O.G. Mouritsen. 1991. Monte Carlo simulation studies of lipid order parameter profiles near integral membrane proteins. *Biophys. J.* 59:261–270.

Swaisgood, M., and M. Schindler. 1989. Lateral diffusion of lectin receptors in fibroblast membranes as a function of cell shape. *Exp. Cell Res.* 180:515–528.

Tomishige, M., and A. Kusumi. 1999. Compartmentalization of the erythrocyte membrane by the membrane skeleton: intercompartmental hop diffusion of band 3. *Mol. Biol. Cell.* 10:2475–2479.

Tomishige, M., Y. Sako, and A. Kusumi. 1998. Regulation mechanism of the lateral diffusion of band 3 in erythrocyte membranes by the membrane skeleton. *J. Cell Biol.* 142:989–1000.

Varma, R., and S. Mayor. 1998. GPI-anchored proteins are organized in submicron domains at the cell membrane. *Nature.* 394:798–801.

Wier, M.L., and M. Edidin. 1986. Effects of cell density and extracellular matrix on the lateral diffusion of major histocompatibility antigens in cultured fibroblasts. *J. Cell Biol.* 103:215–222.

Downloaded from http://rupress.org/jcb/article-pdf/157/6/1071/1304489/jcb15761071.pdf by guest on 28 September 2022